Discrimination of Cognate and Noncognate Substrates at the Active Site of Class II Lysyl-tRNA Synthetase†

Sandro F. Ataide and Michael Ibba*

Department of Microbiology, The Ohio State University, Columbus, Ohio 43210-1292

Received May 10, 2004; Revised Manuscript Received July 12, 2004

ABSTRACT: Within the two unrelated aminoacyl-tRNA synthetase classes, lysyl-tRNA synthetase (LysRS) is the only example known to exist in both classes. To probe the role of the amino acids responsible for L-lysine binding in the active site of the class II LysRS (LysRS2), we studied the *lysS*-encoded *Escherichia coli* protein. On the basis of the structure of L-lysine complexed with *E. coli* LysRS2 (*lysS*), residues implicated in amino acid recognition and discrimination were systematically replaced. Steady-state kinetic parameters for these variants showed reductions in the catalytic efficiency (k_{cat}/K_M) of 1−3 orders of magnitude, allowing the assignment of specific roles for key residues in the active site of LysRS2. To further investigate the role of each residue in discrimination against noncognate amino acids, steady-state kinetic parameters were determined for the nonprotein amino acid *S*-(2-aminoethyl)-L-cysteine, a potent inhibitor of LysRS2. While a number of variants showed reductions of several hundred-fold in efficiency of *S*-(2-aminoethyl)-L-cysteine utilization, this was uniformly accompanied by similar reductions in the efficiency of lysine utilization. Thus, manipulation of the amino acid binding site only allowed up to a 4-fold improvement in *S*-(2-aminoethyl)-L-cysteine discrimination. This is in contrast to the highly effective discrimination against *S*-(2-aminoethyl)-L-cysteine by class I LysRS and correlates with the fundamentally different roles of conserved aromatic residues in the two LysRS active sites. This now provides a mechanistic basis for the proposal that differences in amino acid discrimination have been pivotal in the evolution of two unrelated LysRSs.

The genetic code is based on the correct translation of each codon to its cognate amino acid. One key step in ensuring accuracy during the translation of genetic information is the correct attachment of an amino acid to its cognate tRNA by the aminoacyl-tRNA synthetase (aaRS)[1] family of enzymes. The process of forming a correctly paired aa-tRNA requires that each aaRS selectively bind its respective amino acid, ATP, and the cognate tRNA. Aminoacylation of tRNA is a two-step reaction: the first is the activation reaction, in which the aminoacyl-adenylate is formed, followed by the second step where transfer of the amino acid to the tRNA occurs (*1*, *2*). While aminoacylation is generally highly accurate, some aaRSs must also proofread and edit misacylated tRNA to maintain the accuracy of aa-tRNA synthesis (*3*, *4*).

The aaRS family is divided into two structurally unrelated classes, I and II, with 10 members in each (*5*). The divergent structures lead to functional differences with respect to ATP and tRNA binding in each class (*6*, *7*). An aaRS from each class is designated to each amino acid with only one exception known to date, lysyl-tRNA synthetase [LysRS (*8*)], for which examples from both class I (LysRS1) and class II (LysRS2) are known. Analysis of the distribution of LysRS has so far shown that LysRS2 is found in all eukaryotes, most bacteria, and some archaea, and LysRS1 is present in some bacteria and most archaea (*9*−*11*). LysRS1 and LysRS2 are not generally found together, their coexistence being restricted to a few organisms (*12*). Although structurally different, LysRS1 and LysRS2 are able to recognize lysine and $tRNA^{Lys}$ in vivo and in vitro in much the same way (*9*, *13*, *14*). For example, the elements recognized by both LysRS1 and LysRS2 in $tRNA^{Lys}$ are the same, namely, the anticodon, acceptor stem, and discriminator bases (*13*). This illustrates how the unrelated forms of LysRS perform the same cellular function using different molecular mechanisms for $tRNA^{Lys}$ recognition (*15*). In contrast, the activation mechanism for lysine is significantly different between each LysRS. LysRS2 forms lysyladenylate after binding only lysine and ATP, while LysRS1 additionally requires the prior binding of $tRNA^{Lys}$ (*13*). tRNA binding prior to amino acid activation is a feature shared by only a small subgroup of class I aaRS (*16*−*18*).

The crystal structures of LysRS1 and LysRS2 complexed with lysine reveal that while the mechanisms of recognition of the R group of L-lysine rely on similar arrangements of amino acids in each binding pocket, the active sites are different (*14*, *19*). These structural differences lead to divergent patterns in noncognate substrate discrimination between LysRS1 and LysRS2 (*14*, *15*, *19*). On the basis of comparisons of crystal structures and discrimination of lysine analogues by both LysRSs, we decided to investigate the

† This work was supported by Grant GM 65183 from the National Institutes of Health.

* To whom correspondence should be addressed. Phone: 614-292-2120. Fax: 614-292-8120. E-mail: ibba.1@osu.edu.

[1] Abbreviations: aa-tRNA, aminoacyl-tRNA; aaRS, aminoacyl-tRNA synthetase; AEC, *S*-(2-aminoethyl)-L-cysteine; AspRS, aspartyl-tRNA synthetase; LysRS, lysyl-tRNA synthetase; SA, 5′-*O*-[*N*-(L-lysyl)-sulfamoyl]adenosine.

10.1021/bi0490542 CCC: $27.50
Published on Web 08/27/2004

role of the key residues in the active site of LysRS2 (*lysS* encoded) from *Escherichia coli*. The LysRS2 variants used in this work were designed to evaluate both the recognition of L-lysine and the discrimination of substrate analogues. The assignment of function to each residue studied indicated a specific pattern of binding and discrimination of L-lysine by LysRS2 distinct from LysRS1. In particular, the inherent inability of LysRS2 to discriminate the near cognate amino acid *S*-(2-aminoethyl)-L-cysteine provided insight into the origin and evolution of the two forms of LysRS.

EXPERIMENTAL PROCEDURES

Bacterial Strains and Plasmids. *E. coli lysS*-encoded LysRS2 cloned into the pTYB1 vector (*15*) was used as a template for development of LysRS2 variants. Sets of two complementary primers with 27 nucleotides were designed to encode each desired point mutation. The LysRS2 variants used here are G216A, E240D, E240Q, E278D, E278Q, Y280F, Y280S, N424D, N424Q, F426H, F426W, E428D, E428Q. PCR reactions using *Pfu* turbo DNA polymerase (Stratagene) were performed according to the manufacturer's procedure. PCR products were digested with *Dpn*I (New England BioLabs) and transformed into DH5α cells. Point mutations were confirmed by sequencing each gene completely.

Substrates. *S*-(2-Aminoethyl)-L-cysteine was from Sigma-Aldrich and 5′-*O*-[*N*-(L-lysyl)sulfamoyl]adenosine from RNATEC (Leuven, Belgium). L-[U-^{14}C]Lysine (310 mCi/mmol), L-[U-^{3}H]lysine (85.2 Ci/mmol), and [^{32}P]inorganic pyrophosphate (PP_i, 2.33 Ci/mmol) were from Perkin-Elmer Life Sciences.

Lysyl-tRNA Synthetase Purification. The *E. coli lysS*-encoded LysRS2 and mutants cloned into the pTYB1 vector were expressed in *E. coli* BL21(DE3) cells as described previously (*15*). Cells were harvested by centrifugation and washed in column buffer (20 mM Tris-HCl, pH 8, 500 mM NaCl, 1 mM $MgCl_2$, 10% glycerol). Cells were resuspended in column buffer supplemented with protease inhibitor (Hoffman-La Roche), passed through a French pressure cell, and then centrifuged at 20000*g* for 30 min. The resulting supernatant was loaded onto a chitin affinity bead column (New England Biolabs) according to the manufacturer's instructions. Protein was eluted from the chitin affinity column in a buffer of 50 mM Tris-HCl (pH 8), 1 mM $MgCl_2$, 50 mM NaCl, 10% glycerol, and 10 mM 2-mercaptoethanol. The fractions containing LysRS2 (judged to be >99% pure by Coomassie blue staining after SDS−PAGE) were pooled, concentrated by ultrafiltration using Amicon Ultra-15 (Millipore), dialyzed against storage buffer (50 mM Tris-HCl, pH 8, 1 mM $MgCl_2$, 10% glycerol, 10 mM 2-mercaptoethanol), and stored at −80 °C. The concentration of LysRS2 was determined by active site titration as previously described (*20*) with [^{14}C]-L-lysine, and the reaction was performed for 10 min. Calculations were based on half-of-the-sites reactivity for *E. coli* LysRS (*21*).

Aminoacylation Assays. Aminoacylation was performed at 37 °C in 100 mM Hepes (pH 7.2), 25 mM KCl, 10 mM $MgCl_2$, 4 mM DTT, 5 mM ATP, 5 μM $tRNA^{Lys}$, 2 mM [^{3}H]-L-lysine, and 10−250 nM LysRS2. For the L-Lys K_M determination, all of the concentrations were fixed, but [^{14}C]-L-Lys or [^{3}H]-L-Lys was added at concentrations varying between 0.2 and 5 times K_M. The same procedure was followed for the ATP K_M determination, in which ATP was added at concentrations varying between 0.2 and 5 times the K_M. Aliquots of 10 μL were taken every 15−60 s and spotted onto 3MM filter disks presoaked in 5% TCA (w/v) containing 0.5% (w/v) [^{12}C]-L-Lys. Sample disks were washed, and radioactivity was counted as described previously (*15*).

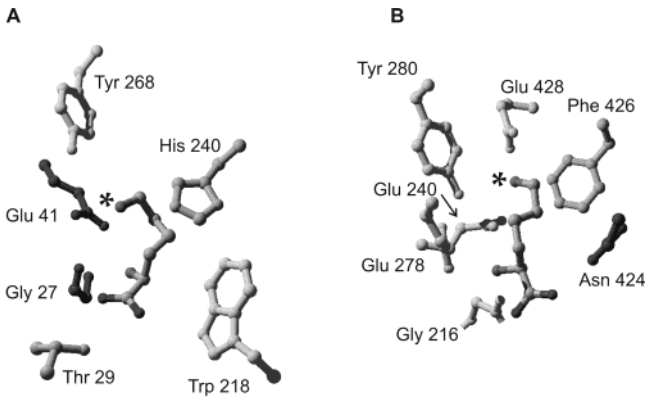

FIGURE 1: (A) L-Lysine in the active site of *Pyrococcus horikoshii* LysRS1. (B) L-Lysine in the active site of *E. coli* LysRS2. The asterisk indicates the ϵ-amino group of the substrate L-lysine molecule.

K_i Determination. To determine K_is for *S*-(2-aminoethyl)-L-cysteine (AEC) and 5′-*O*-[*N*-(L-lysyl)sulfamoyl]adenosine (SA), at least five different concentrations of analogues were first screened in the aminoacylation reaction for each variant under standard conditions with K_M concentrations of [^{14}C]-L-Lys for each LysRS2 variant. Analogue concentrations were then established at which the initial rate of aminoacylation was decreased by 20−50% when compared with the reaction lacking analogue, and these levels were used for K_i determinations. The K_is presented are the average of at least two independent experiments where values deviated by no more than 10% between individual determinations.

ATP−PP_i Exchange Reaction. The ATP−PP_i exchange reaction was performed in 100 mM Hepes (pH 7.2), 15 mM $MgCl_2$, 5 mM ATP, 5 mM [^{32}P]PP_i, 10−300 nM LysRS2, and AEC or lysine concentrations varying from 0.2 to 5 times the K_M for each LysRS2 variant. The reaction mixture was preincubated for 2 min at 37 °C, and then enzyme was added. Twenty-five microliters of the reaction was added to 970 μL of quenching solution [5.6% (v/v) perchloric acid, 1% Norit A, and 75 mM PP_i] at different time points. ATP adsorbed on charcoal was filtered over Whatman GF/C filter disks, washed, and dried, and the level of [^{32}P]ATP was quantified by addition of liquid scintillant (Ultima Gold, Packard Corp.) and scintillation counting.

RESULTS

Selection and Characterization of LysRS2 Variants. On the basis of comparisons between the crystal structures of the LysRS1 and LysRS2 active sites complexed with L-lysine (*14*, *19*), several residues were replaced in LysRS2 from *E. coli* (*lysS* encoded). Substitutions were made with the general aims of assigning specific roles for each position and comparing the roles of synonymous residues in the active sites of LysRS1 and LysRS2 (*15*; Figure 1). The G216A

Table 1: Steady-State Aminoacylation Kinetics of *E. coli* LysRS2 (*lysS* Encoded) with Lys and ATP

LysRS	K_M (μM)	k_{cat} (s^{-1})	k_{cat}/K_M (R)[a]
Lys			
wild type	2.6 ± 0.2	1.8 ± 0.02	1
G216A	196 ± 16	3.4 ± 0.1	33
E240D	3.3 ± 0.3	0.086 ± 0.002	33
E240Q	3.6 ± 0.4	0.0087 ± 0.0004	330
E278D	254 ± 21	0.16 ± 0.006	1100
E278Q	1.4 ± 0.1	0.015 ± 0.003	50
Y280F	24 ± 2	0.031 ± 0.001	500
Y280S	114 ± 16	1.6 ± 0.07	50
N424D	5.2 ± 0.6	1.6 ± 0.07	2.5
N424Q	52 ± 4	0.65 ± 0.01	50
F426H	203 ± 17	2.4 ± 0.08	50
F426W	16 ± 2	0.60 ± 0.01	20
E428D	22 ± 2	1 ± 0.03	14
E428Q	1.3 ± 0.1	0.0200 ± 0.0006	50
ATP			
wild type	12 ± 1.1	3.4 ± 0.2	1
G216A	195 ± 21	0.800 ± 0.02	100
E240D	11 ± 1	0.14 ± 0.003	25
E240Q	14 ± 1	0.013 ± 0.0004	330
E278D	16 ± 2	0.054 ± 0.004	100
E278Q	7.8 ± 0.9	0.017 ± 0.0007	130
Y280F	62 ± 6	0.17 ± 0.005	100
Y280S	147 ± 14	0.35 ± 0.008	130
N424D	21 ± 2	1 ± 0.04	5
N424Q	830 ± 120	2.2 ± 0.09	110
F426H	19 ± 1	0.67 ± 0.01	10
F426W	110 ± 8	2.4 ± 0.08	13
E428D	20 ± 2	1 ± 0.05	5
E428Q	7.8 ± 0.9	0.017 ± 0.0002	130

[a] Relative decrease compared to wild type.

substitution was designed to disrupt the interaction of the main chain carboxylic group of glycine with the α-NH_2 group from lysine. All of the glutamic acid residues in the active site, E240, E278, and E428, were mutated to aspartic acid to evaluate the role of the correct positioning of the carboxylate in the active site and to glutamine to evaluate the effect of a neutral residue. N424 was replaced by aspartic acid, which has the ability to develop a negative charge, and glutamine that allowed evaluation of the role of the correct positioning of this H-bond interaction with the α-carboxyl of lysine. Y280 was evaluated by replacing it with serine, in which the OH group was still present but the aromatic ring is missing, which allows the evaluation of the correct positioning of the OH group at this position. The H-bond interaction between the OH group from Y280 and the ϵ-NH_2 from lysine was investigated by replacing Y280 with phenylalanine. The main hydrophobic residue F426 was replaced by tryptophan, to investigate the effect that a larger hydrophobic molecule will cause in the active site, and by histidine, to evaluate the effect of introducing a possible positive charge in the hydrophobic side of the active site of LysRS2. The replacements of F426 were also intended to make the active site of LysRS2 more similar to LysRS1 (*15*), which contains both a tryptophan and a histidine at the corresponding side relative to lysine.

The effect of each replacement in the active site of LysRS2 on the steady-state kinetics of the aminoacylation reaction was determined. Comparison of the catalytic efficiency (k_{cat}/K_M) of the LysRS2 variants with the wild type indicated that all are less efficient than wild type (Table 1). The K_M for L-lysine and ATP increased from 1.2- to 95-fold for most of the LysRS2 variants when compared to wild type. Only E278Q and E428Q showed decreases of about 2-fold in the K_M values for lysine and ATP. In most cases the increase in K_M was always more significant for L-lysine than for ATP, particularly for G216A, E278D, and F426H, which showed increases of 75-, 98-, and 78-fold, respectively. N424Q was the only mutant to have a significantly higher K_M for ATP, with a 69-fold increase. The k_{cat} values for lysine and ATP were lower than wild type for all mutants except G216A and F426H, which showed increases of 1.8- and 1.3-fold for lysine and decreases of 4- and 5-fold for ATP, respectively. Severe losses in k_{cat} were found for E240Q and E278Q, with decreases of 125- and 212-fold for lysine and 200- and 277-fold for ATP, respectively. Overall, the kinetic parameters for L-lysine and ATP during aminoacylation are in agreement with predictions based on the crystal structure, showing that certain replacements interfere with lysine and/or ATP binding and catalysis.

Discrimination of Lysine Analogues by LysRS2 Variants. We recently reported that LysRS1 and LysRS2 discriminate cognate and noncognate lysine analogues differently (*15*). The strongest inhibitor of both enzymes was 5′-*O*-[*N*-(L-lysyl)sulfamoyl]adenosine (SA), a nonhydrolyzable analogue of lysyladenylate equally effective against both LysRS1 and LysRS2. In contrast, the lysine analogue *S*-(2-aminoethyl)-L-cysteine (AEC) showed a marked difference in apparent affinity, the K_i being approximately 300-fold lower for LysRS2 than LysRS1. To test the possibility that some of the LysRS2 variants developed in this study transformed the active site of LysRS2 into a form mimicking the LysRS1 active site, the K_is for AEC and SA were determined and compared to wild type (Table 2). The inhibition patterns displayed by all of the LysRS2 mutants (with one exception) clearly suggest competitive inhibition by SA and AEC, since K_M but not k_{cat} values changed significantly on addition of analogue. The most significant changes in K_i for SA were observed with Y280F and F426H, which showed 10- and 50-fold increases, respectively. For AEC, the variants showing the most pronounced change in K_i, to values similar to wild-type LysRS1, were G216A, E278D, and F426H, with increases of 317-, 331-, and 335-fold, respectively. Interestingly, Y280S was the only variant to present a mixed pattern of inhibition, since it showed k_{cat} decreases of 7- and 5.3-fold for SA and AEC, and K_i increases of 8- and 90-fold for SA and AEC. Only N424Q had moderate decreases in K_i, 2.5-fold for both SA and AEC.

Activation of AEC. To evaluate changes in substrate specificity associated with perturbed binding and activation of AEC and lysine in the active site of each variant, steady-state kinetic parameters were measured for the ATP−PP_i exchange reaction (Table 3). G216A, E278D, and Y280S showed the most significant increases in the K_M values, 142-, 48-, and 384-fold for AEC and 106-, 239-, and 75-fold for lysine, respectively, compared to wild type. The k_{cat} for AEC and lysine activation was reduced for all replacements, and consequently, the catalytic efficiency of the LysRS2 variants in activating AEC is consistently lower than wild type. Thus G216A, E278D, and Y280S are the least active enzymes with 476-, 1754-, and 1010-fold decreases, respectively (Table 3), in k_{cat}/K_m for AEC activation. In the case of lysine activation, the least active enzymes are G216A, E278D, Y280F, and F426H with 413-, 1000-, 667-, and 923-fold decreases, respectively, in k_{cat}/K_m. Comparison of the dif-

Table 2: Kinetic Parameters for the Inhibition of Steady-State Aminoacylation by *E. coli* LysRS2 (*lysS* Encoded) in the Presence of SA or AEC

LysRS	K_i (μM)	k_{cat} (R)[a]	K_i(variant)/ K_i(wild type)
SA			
wild type	0.028 ± 0.003	0.90 ± 0.03	1
G216A	0.059 ± 0.007	0.29 ± 0.02	2
E240D	0.029 ± 0.003	0.60 ± 0.03	1
E240Q	0.010 ± 0.001	1.5 ± 0.01	0.4
E278D	0.041 ± 0.009	2.3 ± 0.04	1.5
E278Q	0.023 ± 0.004	0.50 ± 0.02	0.8
Y280F	0.27 ± 0.04	1.9 ± 0.02	10
Y280S	0.22 ± 0.03	0.13 ± 0.01	8
N424D	0.039 ± 0.005	0.77 ± 0.04	1
N424Q	0.055 ± 0.006	1.2 ± 0.03	2
F426H	1.3 ± 0.15	0.50 ± 0.01	50
F426W	0.050 ± 0.007	0.82 ± 0.06	2
E428D	0.061 ± 0.009	0.83 ± 0.03	2
E428Q	0.011 ± 0.001	1.1 ± 0.05	0.4
AEC			
wild type	3.9 ± 0.4	0.80 ± 0.02	1
G216A	1240 ± 140	0.39 ± 0.01	300
E240D	3.1 ± 0.7	0.84 ± 0.03	0.8
E240Q	5.4 ± 0.7	1.5 ± 0.02	1
E278D	1290 ± 160	1.8 ± 0.01	300
E278Q	5.0 ± 0.9	0.48 ± 0.03	1
Y280F	72 ± 8	2.1 ± 0.06	20
Y280S	340 ± 60	0.15 ± 0.01	90
N424D	4.0 ± 0.5	0.72 ± 0.04	1
N424Q	76 ± 8	1.2 ± 0.03	20
F426H	1310 ± 170	0.46 ± 0.01	300
F426W	25 ± 3	0.74 ± 0.01	6
E428D	34 ± 7	0.79 ± 0.04	9
E428Q	1.5 ± 0.2	1.1 ± 0.07	0.4

[a] Relative to k_{cat} values determined in the absence of inhibitor (Table 1).

Table 3: Steady-State ATP−PP_i Exchange Kinetics of *E. coli* LysRS2 (*lysS* Encoded) with Lys and AEC

LysRS	K_M (μM)	k_{cat} (s^{-1})	k_{cat}/K_M ($s^{-1}\mu M^{-1}$)	$(k_{cat}/K_M^{Lys})/(k_{cat}/K_M^{AEC})$
Lys				
wild type	43 ± 4	50 ± 0.6	1.2	
G216A	4580 ± 530	14 ± 0.7	0.0029	
E240D	12 ± 1.4	1.6 ± 0.05	0.13	
E240Q	22 ± 3	0.210 ± 0.001	0.0097	
E278D	10300 ± 990	2.1 ± 0.5	0.0012	
E278Q	25 ± 2	0.36 ± 0.01	0.014	
Y280F	2980 ± 310	5.3 ± 0.2	0.0018	
Y280S	3250 ± 460	15 ± 0.7	0.0047	
N424D	137 ± 20	7.8 ± 0.2	0.057	
N424Q	326 ± 42	1.3 ± 0.06	0.041	
F426H	1950 ± 320	2.6 ± 0.01	0.0013	
F426W	80 ± 7	4.6 ± 0.1	0.058	
E428D	215 ± 17	14 ± 0.4	0.065	
E428Q	12 ± 1.6	0.99 ± 0.04	0.079	
AEC				
wild type	14 ± 1.8	7.7 ± 0.02	0.55	2.1
G216A	1980 ± 290	2.2 ± 0.1	0.0011	2.7
E240D	7.2 ± 1	0.44 ± 0.01	0.061	2.2
E240Q	7.4 ± 0.7	0.057 ± 0.0001	0.0077	1.3
E278D	665 ± 95	0.21 ± 0.001	0.00031	3.8
E278Q	5.3 ± 0.6	0.051 ± 0.0001	0.0096	1.5
Y280F	82 ± 12	0.08 ± 0.0003	0.00098	1.8
Y280S	5350 ± 760	2.9 ± 0.01	0.00055	8.5
N424D	9.3 ± 1.8	1.7 ± 0.1	0.18	0.31
N424Q	49 ± 8	0.37 ± 0.001	0.0076	5.4
F426H	261 ± 33	3.2 ± 0.1	0.012	0.11
F426W	11 ± 1.6	1.2 ± 0.03	0.11	0.53
E428D	160 ± 19	5.5 ± 0.1	0.034	1.9
E428Q	12 ± 1.2	0.24 ± 0.008	0.021	3.9

ferences in catalytic efficiency for AEC and lysine displayed by the LysRS2 variants shows that none have acquired a significant improvement in their ability to discriminate lysine from AEC. For most LysRS variants, lysine specificity [defined as $(k_{cat}/K_m^{Lys})/(k_{cat}/K_m^{AEC})$] remained comparable to wild type (Table 3). A 4-fold increase in specificity for lysine was displayed by Y280S relative to wild type, while N424D, F426H, and F426W showed 7-, 19-, and 4-fold decreases compared to AEC. Thus, while inhibitor data clearly showed decreases in apparent affinities for AEC, these were accompanied by decreased efficiencies in lysine utilization and consequently little change in substrate specificity.

DISCUSSION

Specific Recognition of Lysine in the LysRS2 Active Site. Structural studies indicate that the active site of *E. coli* LysRS2 undergoes a large conformational change that stabilizes and promotes effective binding of L-lysine, with the positions of several residues modified significantly (*19*). Interpretations of the effect of mutations on kinetic parameters assume that the mutations only affect local structure and not overall structure of the binding pocket, an assumption generally borne out by the kinetic parameters determined here. For example, G216, whose carboxyl group forms an H-bond with the α-amino group of lysine, is proposed to be part of a loop stabilized by substrate binding. Steady-state kinetic parameters indicate that replacement of G216 does indeed disrupt the H-bond between the α-carboxyl group of residue 216 and the α-amino group of L-lysine. The perturbation of ATP binding suggests that the G216A replacement also disrupts correct repositioning of the corresponding loop (*19*). F426 is also repositioned after lysine binding, with the aromatic ring rotated to presumably promote hydrophobic interaction with the R group of lysine. The substitution F426H disrupted lysine binding, due to insertion of a positively charged residue in the hydrophobic side of the active site. F426W had considerably less impact on lysine binding and, instead, predominantly affected ATP kinetics. Given that neither substitution of F426 would be expected to disrupt the active site H-bond network (Figure 2A−C), it is reasonable to assume that residue 426 contributes to specificity by promoting hydrophobic interactions with the R group of lysine and determining the size of the amino acid binding pocket.

The LysRS2 active site contains three glutamate residues with different proposed roles in substrate recognition. E240 is not directly implicated in lysine binding but is believed to be involved in stabilizing and/or delocalizing the H-bond network by acting as a H-bond donor in the active site. Replacements of E240 for aspartic acid or glutamine had no effect on lysine or ATP binding, but the k_{cat} during the aminoacylation reaction for both mutations was decreased, supporting the proposed indirect role of this residue. In contrast, replacement of E278 by aspartic acid or glutamine had more widespread effects on the kinetics of aminoacylation. The shortening of the side chain in E278D LysRS2 reduced the apparent affinity for lysine, indicating that E278 is directly involved in lysine binding through H-bonding between its carboxyl group and the α-NH_2 of lysine. E278 is in β-strand B3 and does not have the flexibility to be reoriented in the active site when replaced by aspartate (Figure 2D), indicating that this position is devoted to direct

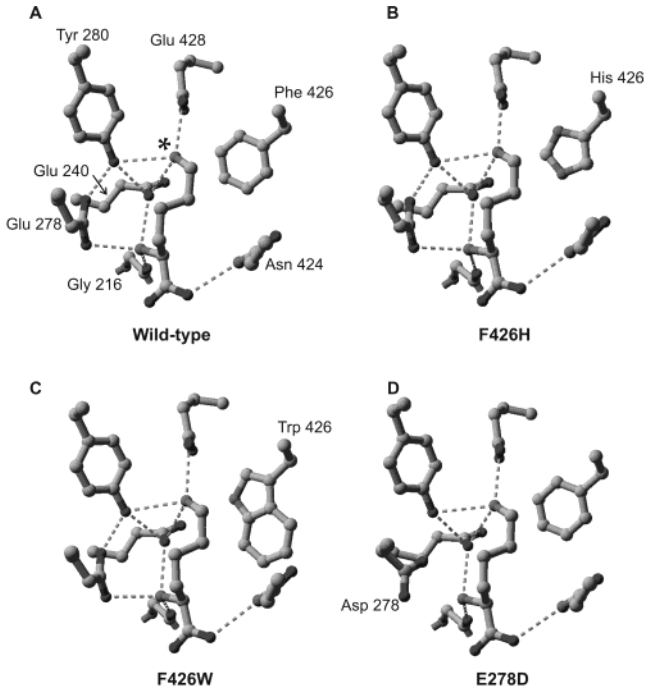

FIGURE 2: L-Lysine recognition by wild-type and variant forms of LysRS2. (A) L-Lysine in the active site of wild-type *E. coli* LysRS2. The asterisk indicates the ϵ-amino group of the substrate L-lysine molecule, and H-bonds are shown as dashed lines. (B−D) Models for the binding of L-lysine to the LysRS2 variants F426H (B), F426W (C), and E278D (D). Residues were modified appropriately, and the resulting structures were energy minimized using Swiss-Pdb Viewer version 3.7. The resulting models were visualized in ball-and-stick representation using MOLMOL version 2k.2 (*23*).

H-bonding with the α-NH_2 of lysine. The E278D replacement was the most detrimental to lysine binding as measured in both the activation and aminoacylation reactions, identifying this as a critical residue in substrate recognition. In contrast, the E278Q replacement had little effect on lysine binding but dramatically reduced k_{cat}. E428 is the final glutamic acid residue in the active site of LysRS2 implicated in the H-bonding network, and it is believed to specifically interact with the ϵ-NH_2 group of lysine. While less dramatic than the changes observed for E278, replacements of E428 followed a similar pattern, indicating that H-bonds mediated by this residue are important for catalysis. The general pattern presented by these replacements is that, at any position in the active site of LysRS2 occupied by glutamic acid, a change to a neutral residue of similar size and H-bonding capacity leads to a reduction in k_{cat}. Amino acid binding is most severely disrupted in E278D, indicating that this residue is essential for binding and positioning of lysine in the active site. This is in agreement with earlier studies of the closely related subclass IIb enzyme aspartyl-tRNA synthetase (AspRS), where the analogous motif 2 residue (D342 in the yeast cytoplasmic enzyme) forms essential interactions with the α-NH_2 group of the substrate aspartic acid (*22*).

Kinetic analyses showed that other active site residues also contribute directly to lysine binding. Substitutions of Y280 indicated that the H-bond between the side chain OH group and the ϵ-NH_2 of lysine is important to promote both substrate binding and catalysis. Replacements at N424 showed that this residue contributes to both lysine and ATP binding and that it is the precise placement, rather than the exact nature, of the H-bonding partner that is critical.

Substrate Specificity Determinants in LysRS2. The availability of numerous variants with changes in cognate amino acid binding provided a basis to probe substrate specificity and discrimination in LysRS2. The effectiveness of inhibition by AEC closely correlated with the efficiency of lysine utilization in all of the LysRS2 variants studied, providing further support for the roles of various residues as described above. Inhibition kinetics for the reaction intermediate analogue SA revealed surprisingly little effect for most of the replacements, suggesting that the majority of the residues studied here are primarily involved in initial substrate recognition and activation (Table 2). While many of the LysRS2 variants displayed significant losses in apparent affinity for the noncognate AEC, in only three cases did this result in a significant change in substrate specificity compared to the cognate substrate lysine. N424D and F426H, both of which would be expected to be in close proximity to the sulfur moiety of AEC, displayed reduced discrimination of lysine versus AEC while Y280S showed a 4-fold increase in specificity. The increase in specificity shown by Y280S compared to wild type indicates that removal of the aromatic ring can cause substantial disruption of the active site, as also suggested by the observation of mixed inhibition kinetics exclusively for this variant.

Divergent Mechanisms of Substrate Discrimination in LysRS1 and LysRS2. The evolution of two unrelated structures to perform the same reaction is so far limited to LysRS among the aaRSs. We previously proposed that the active site of LysRS2 is more open, and therefore able to accommodate lysine analogues more easily, than LysRS1. Our present findings support this suggestion and indicate in more detail how this impacts LysRS2's potential to discriminate certain noncognate amino acids. For example, replacements of F426 were designed with the intention of mimicking analogous residues in the LysRS1 active site and were initially expected to improve rather than lessen specificity as was in fact observed. The F426H replacement had significant effects on cognate and noncognate amino acid binding, indicating that introduction of the imidazole ring may have resulted in electrostatic repulsion of substrates. More generally, our data indicate how insertion of a positive charge in the active site of LysRS2 disrupts substrate binding and similarly how the removal of negative charge (as in the E → Q replacements) diminishes catalytic capacity. A similar pattern was also observed during evaluation of the closely related AspRS active site (*22*), where insertion of a negatively charged residue disrupts interactions with the substrate aspartic acid. In the case of yeast AspRS the key residue is Arg485, which corresponds to E428 in LysRS2. To achieve its selectivity and specificity, AspRS relies on a positively charged active site to interact with aspartic acid, and we can now conclude that the active site architecture of LysRS2 is also reliant on electrostatic interactions for function.

Previous structural studies and the findings described here indicate that LysRS2 uses electrostatic interactions to bind lysine in a more acidic active site than does LysRS1. In contrast to LysRS2 the presence of histidine in the LysRS1 active site does not disrupt interactions with lysine but instead excludes AEC as previously suggested by molecular modeling. The reduced role of electrostatic interactions in LysRS1 is also evident from the presence of only one glutamate residue compared to the three found in the LysRS2 active

site. These fundamental differences between the LysRS1 and LysRS2 active sites now provide a mechanistic basis for their markedly different capacities to discriminate certain substrates.

ACKNOWLEDGMENT

We thank Jeff Levengood, Mette Prætorius-Ibba, and Lau Sennels for critical reading of the manuscript.

REFERENCES

1. Ibba, M., and Söll, D. (2000) Aminoacyl-tRNA synthesis, *Annu. Rev. Biochem. 69*, 617−650.
2. Francklyn, C., Perona, J. J., Puetz, J., and Hou, Y. M. (2002) Aminoacyl-tRNA synthetases: versatile players in the changing theater of translation, *RNA 8*, 1363−1372.
3. Ibba, M., Becker, H. D., Stathopoulos, C., Tumbula, D. L., and Söll, D. (2000) The adaptor hypothesis revisited, *Trends Biochem. Sci. 25*, 311−316.
4. Hendrickson, T. L., and Schimmel, P. (2003) Transfer RNA-dependent amino acid discrimination by aminoacyl-tRNA synthetases, in *Translation Mechanisms* (Lapointe, J., and Brakier-Gingras, L., Eds.) pp 34−64, Kluwer Academic/Plenum Publishers, New York.
5. Cusack, S. (1997) Aminoacyl-tRNA synthetases, *Curr. Opin. Struct. Biol. 7*, 881−889.
6. Arnez, J. G., and Moras, D. (1997) Structural and functional considerations of the aminoacylation reaction, *Trends Biochem. Sci. 22*, 211−216.
7. Ribas De Pouplana, L., and Schimmel, P. (2001) Two classes of tRNA synthetases suggested by sterically compatible dockings on tRNA acceptor stem, *Cell 104*, 191−193.
8. Ibba, M., Morgan, S., Curnow, A. W., Pridmore, D. R., Vothknecht, U. C., Gardner, W., Lin, W., Woese, C. R., and Söll, D. (1997) A euryarchaeal lysyl-tRNA synthetase: resemblance to class I synthetases, *Science 278*, 1119−1122.
9. Söll, D., Becker, H. D., Plateau, P., Blanquet, S., and Ibba, M. (2000) Context-dependent anticodon recognition by class I lysyl-tRNA synthetases, *Proc. Natl. Acad. Sci. U.S.A. 97*, 14224−14228.
10. Ambrogelly, A., Korencic, D., and Ibba, M. (2002) Functional annotation of class I lysyl-tRNA synthetase phylogeny indicates a limited role for gene transfer, *J. Bacteriol. 184*, 4594−4600.
11. O'Donoghue, P., and Luthey-Schulten, Z. (2003) On the evolution of structure in aminoacyl-tRNA synthetases, *Microbiol. Mol. Biol. Rev. 67*, 550−573.
12. Polycarpo, C., Ambrogelly, A., Ruan, B., Tumbula-Hansen, D., Ataide, S. F., Ishitani, R., Yokoyama, S., Nureki, O., Ibba, M., and Söll, D. (2003) Activation of the pyrrolysine suppressor tRNA requires formation of a ternary complex with class I and class II lysyl-tRNA synthetases, *Mol. Cell 12*, 287−294.
13. Ibba, M., Losey, H. C., Kawarabayasi, Y., Kikuchi, H., Bunjun, S., and Söll, D. (1999) Substrate recognition by class I lysyl-tRNA synthetases: a molecular basis for gene displacement, *Proc. Natl. Acad. Sci. U.S.A. 96*, 418−423.
14. Terada, T., Nureki, O., Ishitani, R., Ambrogelly, A., Ibba, M., Söll, D., and Yokoyama, S. (2002) Functional convergence of two lysyl-tRNA synthetases with unrelated topologies, *Nat. Struct. Biol. 9*, 257−262.
15. Levengood, J. D., Ataide, S. F., Roy, H., and Ibba, M. (2004) Divergence in noncognate amino acid recognition between class I and class II lysyl-tRNA synthetases, *J. Biol. Chem. 279*, 17707−17714.
16. Sherlin, L. D., and Perona, J. J. (2003) tRNA-dependent active site assembly in a class I aminoacyl-tRNA synthetase, *Structure 11*, 591−603.
17. Delagoutte, B., Moras, D., and Cavarelli, J. (2000) tRNA aminoacylation by arginyl-tRNA synthetase: induced conformations during substrates binding, *EMBO J. 19*, 5599−5610.
18. Sekine, S., Nureki, O., Dubois, D. Y., Bernier, S., Chenevert, R., Lapointe, J., Vassylyev, D. G., and Yokoyama, S. (2003) ATP binding by glutamyl-tRNA synthetase is switched to the productive mode by tRNA binding, *EMBO J. 22*, 676−688.
19. Onesti, S., Desogus, G., Brevet, A., Chen, J., Plateau, P., Blanquet, S., and Brick, P. (2000) Structural studies of lysyl-tRNA synthetase: conformational changes induced by substrate binding, *Biochemistry 39*, 12853−12861.
20. Wilkinson, A. J., Fersht, A. R., Blow, D. M., and Winter, G. (1983) Site-directed mutagenesis as a probe of enzyme structure and catalysis: tyrosyl-tRNA synthetase cysteine-35 to glycine-35 mutation, *Biochemistry 22*, 3581−3586.
21. Commans, S., Blanquet, S., and Plateau, P. (1995) A single substitution in the motif 1 of *Escherichia coli* lysyl-tRNA synthetase induces cooperativity toward amino acid binding *Biochemistry 34*, 8180−8189.
22. Cavarelli, J., Eriani, G., Rees, B., Ruff, M., Boeglin, M., Mitschler, A., Martin, F., Gangloff, J., Thierry, J. C., and Moras, D. (1994) The active site of yeast aspartyl-tRNA synthetase: structural and functional aspects of the aminoacylation reaction, *EMBO J. 13*, 327−337.
23. Koradi, R., Billeter, M., and Wüthrich, K. (1996) MOLMOL: a program for display and analysis of macromolecular structures, *J. Mol. Graphics 14*, 29−32.

BI0490542